Indian Journal of Pure & Applied Physics
Vol. 59, January 2021, pp. 28-39

Heat and mass transfer effect of a Magnetohydrodynamic Casson fluid flow in the presence of inclined plate

R Vijayaragavan[a], V Bharathi[b*] & J Prakash[c]

[a]Department of Mathematics, Thiruvalluvar University, Vellore, Tamilnadu, India.

[b]Department of Mathematics, Adhiparasakthi College of Arts and Science (Autonomous) Kalavai, Tamilnadu, India.

[c]Department of Mathematics, Avvaiyar Government College for Women, Karaikal-609 602, Pondicherry –U T, India.

Received 26 March 2020; accepted 14 October 2020

The key purpose of this paper is to study the convection of a transient state in the flow of MHD Casson fluid over an inclined layer. In addition, the influence of the magnetic field, Dufour effects and heat suction / injection through porous medium are considered in the present analysis. By the Laplace transformation process, the analytical solutions of governing equations are established. By using the particular solution of fluid temperature and species concentration, the expressions for Nusselt number and Sherwood number are also premeditated. The variations in fluid velocity, fluid temperature, species concentration, Nusselt number and Sherwood number are shown graphically for different values of pertinent flow parameters. It is noted that with an increase in the Dufour number, the axial velocity decreases and it is also noted that the concentration of the species decreases with an increase in the Dufour number. The velocity decreases as all the cases of cooling and heating of the porous inclined plate raise the suction parameter.

Keywords: Inclined plate, Casson fluid , Dufour effect, thermal radiation, Porous medium, chemical reaction.

1 Introduction

In the Newtonian fluid model many flow characteristics are not explicable, hence the learning of the non Newtonian fluid model is useful. Non Newtonian fluid exerts non-linear interaction between of shear strain and rate of the shear stress. In literature, various models are available for non-Newtonian fluids such as Casson model, Kelvin model, Oldroyd-B model, Burger model, Jeffrey model, Maxwell model, fourth grade model, third grade model, second grade model and some fractional order of viscoelastic models *etc*., and researchers are using these approaches to study new works in fluid dynamics[1-6]. The fluid in Casson is also one of the non-Newtonian fluid. This fluid is very well-known for its various characteristics. The Casson model was introduced for predicting the flow behaviour of pigment-oil suspensions in the Casson fluid[7]. The Alfven wave discovery had completed Alfven's formation as an autonomous science of Magnetohydrodynamic (MHD)[8], while Hartmann[9] studied the laminar flow of an electrically conductive fluid in the presence of homogeneous magnetic fields. Su *et al.*[10] have shown the special effects of an inclined magnetic field on the erratic squeezing flow between suction or injection matching plates. The consistently MHD-free convective chemical reactor fluid flux has been extracted from Okuyade *et al.*[11] through the vertical plate with Dufour, thermal radiation, Soret and steady suction results. MHD flow of a second grade split fluid over an inclined heated flat Chaos solutions and fractals are recorded by Tassaddiq *et al.*[12]. MHD Casson fluid flow with vertical stretching surface was studied by Venkata *et al.*[13].

Recently, there has been a lot of focus to the study of fluid flows and heat transfer by porous medium. It is mostly due to various uses of porous flux, such as storing radioactive nuclear waste products, chemical separation systems, filtration, transpiration cooler, water transport and soil contamination. Examples of normal porous media also include ocean sand, sandstone, calcareous shale, human lung, bile duct and gall bladder in small blood vessels[3-6,14-18]. Pramanik[19] has researched porous heat transfer and Casson fluids in the thermal radiation firm exponentially with an exponentially porous base

*Corresponding author: (E-mail:bharathiv42@gmail.com)

stretch. Double diffusive effects on mixed convection Casson fluid flow with inclined plate can be discovered using the Darcian porous medium by Prasad *et al.*[20]. The study of fluid Casson on a vertical porous surface with a chemical reaction in the Magnetical Field was proposed by Arthur *et al.*[21]. The impact on unstable MHD free convection flows past a wall ramped with inclined layer, through thermal diffusion effects analytically studied by Vijayaragavan *et al.*[22]. The effects of chemical reaction and heat generation or absorption on the fluid flow of MHD Casson in porous medium using ramped wall temperature were also discussed by Kataria *et al.*[23]. Jawad Raza[24] explored the effects of thermal radiation and slip on the hydrodynamic magneto stagnation point flow of the Casson fluid model. In the presence of a temperature gradient dependent heat sink with specified heat and mass flux, Palaniammal *et al.*[25] evaluated MHD viscous Casson fluid flow.

Chemical reaction and thermal diffusion results on unstable MHD free convection with an exponentially accelerated inclined plate were explored by Vijayaragavan *et al.*[26]. Non-uniform heat sink or source and chemical reaction effects on Casson fluid flow over a flat plate saturated with Porous Medium and vertical cone were studied by Vijayalakshmi *et al.*[27]. In the boundary layer study, Ajayi *et al.*[28] made the dissipation effects on the motion of Casson fluid for a paraboloid revolution. The Casson fluid model has been researched by Hamida *et al.*[29] in heat transfer and flow analysis. Casson fluid flow mass and heat transfer over an unsteady Permeable stretching surface derived by Shateyi *et al.*[30] presented Dufour and Soret effects on unsteady Casson magneto-nanofluid flow over an inclined plate used in a porous medium. Exact and mathematical radiated flow computations of Casson nanofluids under heat and mass flux conditions were analytically addressed by Mackolil *et al.*[31]. The numerical analysis of double stratification in Casson fluid flow in the presence of mixed convection and chemical reaction was described by Rehman *et al.*[32]. The effects of viscous dissipation and convective boundary conditions on the magneto hydrodynamics flow of Casson liquid over a deformable porous channel were stated by Neeraja *et al.*[33]. Slip effects on ohmic dissipative non-Newtonian fluid flow were obtained by Renuka *et al.*[34]. Vijayaragavan *et al.*[35] discussed dufour effects of Casson fluid .In porous medium with heat and mass transfer, Das *et al.*[36] reported unsteady MHD chemically reactive double-diffusive Casson fluid past flat plate.

Nevertheless, in the presence of Dufour impact, none of the studies have considered the Casson model for representing the inclined vertical layer. The main object of the present paper is to the study the transient state convection of fluid from MHD Casson over an inclined layer. Furthermore, the effects of the magnetic field, Dufour effects and heat suction / injection through the porous medium are studiedin the present study. Laplace transform technique has been applied to find out the exact solution of the governing equations. This model can be used for the research of free convection flow in the cooling of nuclear reactor or for the study of star and planetary systems.

2 Mathematical Analysis

An unsteady motion of a Casson fluid model with electrically conducting fluid flowing through an endless vertical plaque was taken into consideration for the co-ordinate system in such a method that $\bar{x}$ -axis is along the plate in upward direction, $\bar{y}$-axis normal to the plate and $\bar{z}$ -axis vertical to $\bar{x}\,\bar{y}$-plane. The fluid is allowed by identical transverse magnetic field B_0 applied parallel to $\bar{y}$ axis. We consider at time $\bar{t} \le 0$, both the plate and fluid are at rest and maintained at uniform temperature $\bar{T}_\infty$ and uniform surface concentration $\bar{C}_\infty$. At time $\bar{t} \ge 0$, plate starts moving in $\bar{x}$-direction against the gravitational field with time dependent velocity $\bar{u}$. Temperature of the plate is lowered or raised to $\bar{T}_\infty + (\bar{T}_w - \bar{T}_\infty)\,\bar{t}/t_0$ at $0 \le \bar{t} \le t_0$. Also $t_0 > \bar{t}$, plate is retained at the uniform temperature $\bar{T}_\infty$. Projected Physical model of the problem presented in Fig. 1.

The rheological equation of state for the Cauchy stress tensor of Casson fluid is given by

$$\tau_{ij} = \begin{cases} 2e_{ij}\left(\mu_B + \frac{py}{\sqrt{2\pi}}\right) & \pi > \pi_c \\ 2e_{ij}\left(\mu_B + \frac{py}{\sqrt{2\pi_c}}\right) & \pi < \pi_c \end{cases} \qquad \ldots(1)$$

where rate, $\pi = e_{ij}$ and e_{ij} is the (i, j)th element of the deformation rate, π is the product of the component of deformation rate with itself, π_c is a critical value of this product based on the non-Newtonian model, μ_B is plastic dynamic viscosity of the non-Newtonian fluid

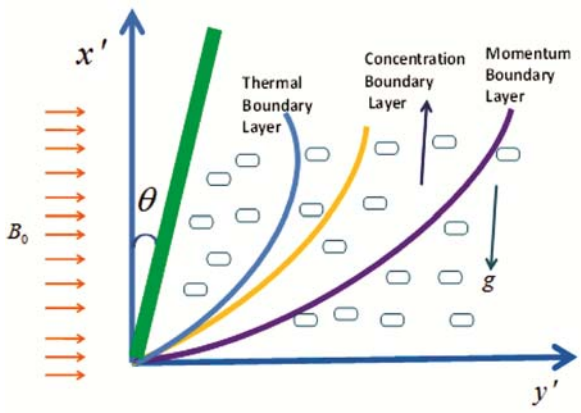

Fig. 1 — Projected Physical model boundary conditions are given below.

and $_{P\,y}$ is yield stress of fluid. Using the above conditions, we get the following velocity temperature and concentration equation with initial and boundary conditions are given below.

$$\frac{\partial \bar{u}}{\partial \bar{t}} = \frac{\mu}{\rho}\left(1+\frac{1}{\Omega}\right)\frac{\partial^2 \bar{u}}{\partial \bar{t}^2} - \frac{\mu \bar{u}}{\rho \bar{k}_1} - \frac{\sigma B_0^2 \bar{u}}{\rho} + g_T \cos\alpha\,\beta(\bar{T}-\bar{T}_\infty) + g_C \cos\alpha\,\beta(\bar{C}-\bar{C}_\infty), \quad \ldots(2)$$

$$\frac{\partial \bar{T}}{\partial \bar{t}} = \frac{\kappa}{\rho c_p}\frac{\partial^2 \bar{T}}{\partial \bar{y}^2} - \frac{1}{\rho c_p}\frac{\partial q_r}{\partial \bar{y}} + \frac{D_m k_T}{\rho c_p C_s}\frac{\partial^2 \bar{C}}{\partial \bar{y}^2} + \frac{\bar{Q}_0(\bar{T}-\bar{T}_\infty)}{\rho c_p}, \quad \ldots(3)$$

$$\frac{\partial \bar{C}}{\partial \bar{t}} = D\frac{\partial^2 \bar{C}}{\partial \bar{y}^2} - \bar{k}(\bar{C}-\bar{C}_\infty). \quad \ldots(4)$$

and the boundary conditions for the above fluid flow are given below

$$\left.\begin{aligned} &\bar{u}=0,\ \bar{T}=\bar{T}_\infty, \bar{C}=\bar{C}_\infty \text{ for } \bar{t}\le 0 \text{ and } \bar{y}\ge 0,\\ &\bar{u}=\bar{u}_0\cos(\bar{\omega}\bar{t}), \text{ at } \bar{y}=0 \text{ for } \bar{t}\ge 0,\\ &\bar{T}=T_\infty+(T_w-T_\infty)\frac{u_0^2\bar{t}}{\nu} \text{ at } \bar{y}=0 \text{ for } \bar{t}>0,\\ &\bar{C}=\bar{C}_\infty+(\bar{C}_w-\bar{C}_\infty)\frac{u_0^2\bar{t}}{\nu} \text{ at } \bar{y}=0 \text{ for } \bar{t}>0,\\ &\bar{u}\to 0,\ \bar{T}\to\bar{T}_\infty,\ \bar{C}\to\bar{C}_\infty \text{ at } \bar{y}\to\infty \text{ for } \bar{t}>0 \end{aligned}\right\} \quad \ldots(5)$$

The local gradient for the case of an optically slim gas can be written in the form

$$\frac{\partial q_r}{\partial \bar{y}} = -4\bar{a}\sigma(\bar{T}_\infty^4 - \bar{T}^4) \quad \ldots(6)$$

Here the temperature differences within the flow are suitably small and that T'^4 may be expressed as a linear function of the temperature. To obtained $\bar{T}^4$ expanding Taylor series about T'_∞ and omitting the higher order terms, we get

$$\bar{T}^4 = 4\bar{T}_\infty^3\bar{T} - 3\bar{T}_\infty^4 \quad \ldots(7)$$

Substituting Eq. 6-7 in (3), we get

$$\frac{\partial \bar{T}}{\partial \bar{t}} = \frac{\kappa}{\rho c_p}\frac{\partial^2 \bar{T}}{\partial \bar{y}^2} + \frac{16\bar{a}\sigma\bar{T}_\infty^3}{\rho c_p}(\bar{T}_\infty - \bar{T}) + \frac{D_m k_t}{c_p c_s}\frac{\partial^2 \bar{C}}{\partial \bar{y}^2} - \frac{\bar{Q}_0(\bar{T}-\bar{T}_\infty)}{\rho c_p}. \quad \ldots(8)$$

The dimensionless parameters and variables are defined as follows

$$\left.\begin{aligned} &y=\frac{\bar{y}u_0}{\nu}, u=\frac{\bar{u}}{u_0}, t=\frac{u_0^2\bar{t}}{\nu}, \bar{T}=\frac{\bar{T}-\bar{T}_\infty}{\bar{T}_w-\bar{T}_\infty}, \bar{C}=\frac{\bar{C}-\bar{C}_\infty}{\bar{C}_w-\bar{C}_\infty},\\ &G_r=\frac{g\beta_T\nu(\bar{T}_w-\bar{T}_\infty)}{u_0^3}, G_m=\frac{g\beta_C\nu(\bar{C}_w-\bar{C}_\infty)}{u_0^3}, P_r=\frac{\mu c_p}{\kappa},\\ &Sc=\frac{\nu}{D},\ M=\frac{\sigma B_0^2\nu}{\rho u_0^2},\ R=\frac{16\bar{a}\sigma\nu^2\sigma\bar{T}_\infty^3}{ku_0^2},\ Q=\frac{\nu\bar{Q}_0}{\rho c_p u_0^2},\\ &Du=\frac{D_m k_t(\bar{C}_w-\bar{C}_\infty)}{c_s c_p\nu(\bar{T}_w-\bar{T}_\infty)},\ k=\frac{\nu\bar{k}}{u_0^2}, k_1=\frac{u_0^2\bar{k}_1}{\nu}, \mu=\rho\nu. \end{aligned}\right\} \quad \ldots(9)$$

The dimensionless governing equations can be written as follows.

$$\frac{\partial u}{\partial t} = \left(\frac{1}{1+\Omega}\right)\frac{\partial^2 u}{\partial y^2} - \frac{\left(M^2k_1+1\right)}{k_1}u + G_r\cos\alpha T + G_m\cos\alpha C, \quad \ldots(10)$$

$$\frac{\partial T}{\partial t} = \frac{1}{\Pr}\frac{\partial^2 T}{\partial y^2} - \left(\frac{R}{\Pr}+Q_0\right)T + Du\frac{\partial^2 C}{\partial y^2}, \quad \ldots(11)$$

$$\frac{\partial C}{\partial t} = \frac{1}{Sc}\frac{\partial^2 C}{\partial y^2} - kC. \quad \ldots(12)$$

And the related boundary conditions become

$$\left.\begin{aligned} &u=0,\ T=0,\ C=0 \text{ for } y\ge 0 \quad \text{and } t\le 0\\ &u=\cos(\omega t), C=t, T=t \text{ at } y=0 \quad \text{for } t>0\\ &u\to 0,\ T\to 0,\ C\to 0, \text{ as } y\to\infty \text{ for } t>0 \end{aligned}\right\} \quad \ldots(13)$$

3. The Method of Solution

To get the accurate solution for fluid temperature, fluid velocity and concentration by solving the dimensionless governing equations from (10) to (12) subject to the boundary conditions (13) using Laplace transforms method and after simplification is obtainable in the following form.

$$C=\left(\frac{t}{2}+\frac{y\sqrt{Sc}}{4\sqrt{k}}\right)\exp\left(y\sqrt{k\,Sc}\right)erfc\left(\frac{y\sqrt{Sc}}{2\sqrt{t}}+\sqrt{kt}\right)+\left(\frac{t}{2}-\frac{y\sqrt{Sc}}{4\sqrt{k}}\right)\exp\left(-y\sqrt{k\,Sc}\right)erfc\left(\frac{y\sqrt{Sc}}{2\sqrt{t}}-\sqrt{kt}\right) \quad \ldots (14)$$

$$T=(1-a_5)\left(\frac{t}{2}+\frac{y\,\mathrm{Pr}}{4\sqrt{R+Q_0\,\mathrm{Pr}}}\right)\exp(y\sqrt{R+Q_0\,\mathrm{Pr}})$$
$$erfc\left(\frac{y\sqrt{\mathrm{Pr}}}{2\sqrt{t}}+\sqrt{t(\tfrac{R}{\mathrm{Pr}}+Q_0)}\right)+(1-a_5)\left(\frac{t}{2}-\frac{y\,\mathrm{Pr}}{4\sqrt{R+Q_0\,\mathrm{Pr}}}\right)$$
$$\exp(-y\sqrt{(R+Q_0\,\mathrm{Pr})})\,erfc\left(\frac{y\sqrt{\mathrm{Pr}}}{2\sqrt{t}}-\sqrt{t(\tfrac{R}{\mathrm{Pr}}+Q_0)}\right)$$
$$\exp(-y\sqrt{(R+Q_0\,\mathrm{Pr})})\,erfc\left(\frac{y\sqrt{\mathrm{Pr}}}{2\sqrt{t}}-\sqrt{t(\tfrac{R}{\mathrm{Pr}}+Q_0)}\right)$$
$$-\frac{(a_4-a_6)\exp(-a_2\,t)}{2}\left[\begin{array}{l}\exp(y\sqrt{R+(Q_0-a_2)\,\mathrm{Pr}}\\ erfc\left(\frac{y\sqrt{\mathrm{Pr}}}{2\sqrt{t}}+\sqrt{(\frac{R}{\mathrm{Pr}}+Q_0-a_2)t}\right)\\ +\exp(-y\sqrt{R+(Q_0-a_2)\,\mathrm{Pr}}\\ erfc\left(\frac{y\sqrt{\mathrm{Pr}}}{2\sqrt{t}}-\sqrt{(\frac{R}{\mathrm{Pr}}+Q_0-a_2)t}\right)\end{array}\right]$$
$$+\frac{(a_4-a_2)}{2}\left[\begin{array}{l}\exp(y\sqrt{R+Q_0\,\mathrm{Pr}})\\ erfc\left(\frac{y\sqrt{\mathrm{Pr}}}{2\sqrt{t}}+\sqrt{(R+Q_0\,\mathrm{Pr})t}\right)\\ +\exp(-y\sqrt{R+Q_0\,\mathrm{Pr}})\\ erfc\left(\frac{y\sqrt{\mathrm{Pr}}}{2\sqrt{t}}-\sqrt{(R+Q_0\,\mathrm{Pr})t}\right)\end{array}\right]$$
$$-\frac{(a_4-a_6)}{2}\left[\begin{array}{l}\exp(y\sqrt{kSc})\,erfc\left(\frac{y\sqrt{Sc}}{2\sqrt{t}}+\sqrt{kt}\right)\\ +\exp(-y\sqrt{kSc})\,erfc\left(\frac{y\sqrt{Sc}}{2\sqrt{t}}-\sqrt{kt}\right)\end{array}\right]$$
$$+a_5\left[\begin{array}{l}\left(\frac{t}{2}+\frac{ySc}{4\sqrt{k}}\right)\exp(y\sqrt{kSc})\\ erfc\left(\frac{y\sqrt{Sc}}{2\sqrt{t}}+\sqrt{kt}\right)\\ +\left(\frac{t}{2}-\frac{ySc}{4\sqrt{k}}\right)\exp(-y\sqrt{kSc})\\ erfc\left(\frac{y\sqrt{Sc}}{2\sqrt{t}}-\sqrt{kt}\right)\end{array}\right]$$
$$+\frac{(a_4-a_6)}{2}\exp(-a_2\,t)\left[\begin{array}{l}\exp(y\sqrt{(k-a_2)Sc})\\ erfc\left(\frac{y\sqrt{Sc}}{2\sqrt{t}}+\sqrt{(k-a_2)t}\right)\\ +\exp(-y\sqrt{(k-a_2)Sc})\\ erfc\left(\frac{y\sqrt{Sc}}{2\sqrt{t}}-\sqrt{(k-a_2)t}\right)\end{array}\right] \quad \ldots(15)$$

$$u=\frac{\exp(-i\omega t)}{4}\left[\begin{array}{l}\exp(y\sqrt{b(a-i\omega)})erfc\left(\frac{y\sqrt{b}}{2\sqrt{t}}+\sqrt{(a-i\omega)t}\right)\\ +\exp(-y\sqrt{b(a-i\omega)}\,erfc\left(\frac{y\sqrt{b}}{2\sqrt{t}}-\sqrt{(a-i\omega)t}\right)\end{array}\right]$$
$$+\frac{\exp(i\omega t)}{4}\left[\begin{array}{l}\exp(y\sqrt{b(a+i\omega)}erfc\left(\frac{y\sqrt{b}}{2\sqrt{t}}+\sqrt{(a+i\omega)t}\right)\\ +\exp(-y\sqrt{b(a+i\omega)}\,erfc\left(\frac{y\sqrt{b}}{2\sqrt{t}}-\sqrt{(a+i\omega)t}\right)\end{array}\right]$$
$$+\frac{A_1}{2}\left[\begin{array}{l}\exp(y\sqrt{ab})\;erfc\left(\frac{y\sqrt{b}}{2\sqrt{t}}+\sqrt{at}\right)\\ +\exp(-y\sqrt{ab})\;erfc\left(\frac{y\sqrt{b}}{2\sqrt{t}}-\sqrt{at}\right)\end{array}\right]+$$

$$\frac{A_2}{2}\left[\begin{array}{l}\left(\frac{t}{2}+\frac{y\sqrt{b}}{4\sqrt{a}}\right)\exp(y\sqrt{a})\ erfc\left(\frac{y\sqrt{b}}{2\sqrt{t}}+\sqrt{at}\right)\\+\left(\frac{t}{2}-\frac{y\sqrt{b}}{4\sqrt{a}}\right)\exp(-y\sqrt{a})\,erfc\left(\frac{y\sqrt{b}}{2\sqrt{t}}-\sqrt{at}\right)\end{array}\right]$$

$$+\frac{A_3\exp(-a_2t)}{2}\left[\begin{array}{l}\exp(y\sqrt{b(a-a_2)})erfc\left(\frac{y\sqrt{b}}{2\sqrt{t}}+\sqrt{(a-a_2)t}\right)\\+\exp(-y\sqrt{b(a-a_2)})\,erfc\left(\frac{y\sqrt{b}}{2\sqrt{t}}-\sqrt{(a-a_2)t}\right)\end{array}\right]$$

$$+\frac{A_4\exp(-a_8t)}{2}\left[\begin{array}{l}\exp(y\sqrt{b(a-a_8)})erfc\left(\frac{y\sqrt{b}}{2\sqrt{t}}+\sqrt{(a-a_8)t}\right)\\+\exp(-y\sqrt{b(a-a_8)})\,erfc\left(\frac{y\sqrt{b}}{2\sqrt{t}}-\sqrt{(a-a_8)t}\right)\end{array}\right]$$

$$+\frac{A_5\exp(a_{21}t)}{2}\left[\begin{array}{l}\exp(y\sqrt{b(a-a_{21})}\\erfc\left(\frac{y\sqrt{b}}{2\sqrt{t}}+\sqrt{(a-a_{21})t}\right)\\+\exp(-y\sqrt{b(a-a_{21})}\\erfc\left(\frac{y\sqrt{b}}{2\sqrt{t}}-\sqrt{(a-a_{21})t}\right)\end{array}\right]$$

$$+\frac{A_6}{2}\left[\begin{array}{l}\exp(y\sqrt{\Pr Q_0+R})\,erfc\left(\frac{y\sqrt{\Pr}}{2\sqrt{t}}+\sqrt{(Q_0+R/\Pr)t}\right)\\+\exp(-y\sqrt{\Pr Q_0+R})\,erfc\left(\frac{y\sqrt{\Pr}}{2\sqrt{t}}-\sqrt{(Q_0+R/\Pr)t}\right)\end{array}\right]$$

$$+A_7\left[\begin{array}{l}\left(\frac{t}{2}+\frac{y\Pr}{4\sqrt{P_rQ_0+R}}\right)\exp(y\sqrt{\Pr Q_0+R})\\erfc\left(\frac{y\Pr}{2\sqrt{t}}+\sqrt{(Q_0+\frac{R}{\Pr})t}\right)+\\\left(\frac{t}{2}-\frac{y\Pr}{4\sqrt{P_rQ_0+R}}\right)\exp(-y\sqrt{\Pr Q_0+R})\\erfc\left(\frac{y\Pr}{2\sqrt{t}}-\sqrt{(Q_0+\frac{R}{\Pr})t}\right)\end{array}\right]$$

$$+\frac{A_8\exp(-a_2t)}{2}\left[\begin{array}{l}\exp(y\sqrt{\Pr(Q_0-a_2)+R})\\erfc\left(\frac{y\sqrt{\Pr}}{2\sqrt{t}}+\sqrt{t(\frac{R}{\Pr}+Q0-a2)}\right)\\+\exp(-y\sqrt{\Pr(Q_0-a_2)+R})\\erfc\left(\frac{y\sqrt{\Pr}}{2\sqrt{t}}-\sqrt{t(\frac{R}{\Pr}+Q0-a2)}\right)\end{array}\right]$$

$$+\frac{A_9\exp(-a_8t)}{2}\left[\begin{array}{l}\exp(y\sqrt{R+(a_8-Q_0)\Pr})\\erfc\left(\frac{y\sqrt{\Pr}}{2\sqrt{t}}+\sqrt{(\frac{R}{\Pr}+Q_0-a_8)t}\right)\\+\exp(-y\sqrt{R+(a_8-Q_0)\Pr})\\erfc\left(\frac{y\sqrt{\Pr}}{2\sqrt{t}}-\sqrt{(\frac{R}{\Pr}+Q_0-a_8)t}\right)\end{array}\right]$$

$$+\frac{A_{10}}{2}\left[\begin{array}{l}\exp(y\sqrt{kSc})\,erfc\left(\frac{y\sqrt{Sc}}{2\sqrt{t}}+\sqrt{kt}\right)\\+\exp(-y\sqrt{kSc})\,erfc\left(\frac{y\sqrt{Sc}}{2\sqrt{t}}-\sqrt{kt}\right)\end{array}\right]$$

$$+A_{11}\left[\begin{array}{l}\left(\frac{t}{2}+\frac{y\sqrt{Sc}}{4\sqrt{k}}\right)\exp(y\sqrt{kSc})erfc\left(\frac{y\sqrt{Sc}}{2\sqrt{t}}+\sqrt{kt}\right)+\\\left(\frac{t}{2}-\frac{y\sqrt{Sc}}{4\sqrt{k}}\right)\exp(-y\sqrt{kSc})erfc\left(\frac{y\sqrt{Sc}}{2\sqrt{t}}-\sqrt{kt}\right)\end{array}\right]$$

$$+\frac{A_{12}\exp(-a_2t)}{2}\left[\begin{array}{l}\exp(y\sqrt{(k-a_2)Sc})\,erfc\left(\frac{y\sqrt{S_c}}{2\sqrt{t}}+\sqrt{(k-a_2)t}\right)\\+\exp(-y\sqrt{(k-a_2)Sc})\,erfc\left(\frac{y\sqrt{S_c}}{2\sqrt{t}}-\sqrt{(k-a_2)t}\right)\end{array}\right]$$

$$\frac{A_{13}\exp(-a_{21}t)}{2}\left[\begin{array}{l}\exp(y\sqrt{(k-a_{21})Sc})\\erfc\left(\frac{y\sqrt{S_c}}{2\sqrt{t}}+\sqrt{(k-a_{21})t}\right)\\+\exp(-y\sqrt{(k-a_{21})Sc})\\erfc\left(\frac{y\sqrt{S_c}}{2\sqrt{t}}-\sqrt{(k-a_{21})t}\right)\end{array}\right]$$

...(16)

4 Nusselt Number

The Nusselt number finds from temperature and is specified by $Nu = -\left[\frac{\partial T}{\partial y}\right]_{y=0}$,

$$
\begin{aligned}
&= (1-a_5)\left[\begin{array}{l} t\sqrt{R+Q_0\,\mathrm{Pr}}\left(1-erfc\sqrt{(\frac{R}{\mathrm{Pr}}+Q_0)t}\right) \\ +\exp(-(\frac{R}{\mathrm{Pr}}+Q_0)t)\sqrt{\frac{\mathrm{Pr}\,t}{\pi}}+ \\ \left(1-erfc\sqrt{(\frac{R}{\mathrm{Pr}}+Q_0)t}\right)\frac{P_r}{2\sqrt{R+Q_0\,\mathrm{Pr}}} \end{array}\right] \\
&+(a_4-a_6) \\
&\left[\begin{array}{l} \sqrt{R+Q_0\,\mathrm{Pr}}\left(1-erfc\sqrt{(R+Q_0\,\mathrm{Pr})t}\right)+ \\ \sqrt{\frac{\mathrm{Pr}}{\pi t}}\exp(-(\frac{R}{\mathrm{Pr}}+Q_0)t)-\exp(-a_2\,t)\sqrt{R+(Q_0-a_2)\,\mathrm{Pr}} \\ \left(1-erfc\sqrt{(\frac{R}{\mathrm{Pr}}+Q_0-a_2)t}\right)-\exp(-a_2\,t)\sqrt{\frac{\mathrm{Pr}}{\pi t}} \\ \exp(-(\frac{R}{\mathrm{Pr}}Q_0-a_2)t)-\sqrt{kSc}\left(1-erfc(\sqrt{kt})\right) \\ -\sqrt{\frac{Sc}{\pi t}}\exp(-kt) \end{array}\right] \\
&+a_5\left[\begin{array}{l} t\sqrt{kSc}\left(1-erfc(\sqrt{kt})\right)-\sqrt{\frac{Sc}{\pi t}}\exp(-kt) \\ +\frac{1}{2}\sqrt{\frac{Sc}{k}}\left(1-erfc(\sqrt{kt})\right) \end{array}\right] \\
&+(a_4-a_6) \\
&\left[\begin{array}{l} \exp(-a_2\,t)\sqrt{(k-a_2)Sc}\left(1-erfc(\sqrt{(k-a_2)t})\right) \\ +\exp(-a_2\,t)\sqrt{\frac{Sc}{\pi t}}\exp((k-a_2)t) \end{array}\right]
\end{aligned}
$$

...(17)

5 Sherwood Number

The Sherwood number obtained by concentration field is given in dimensionless form as

$$S_h = \left(t\sqrt{kSc}+\frac{Sc}{2\sqrt{k}}\right)\left(1-erfc(\sqrt{kt})\right) + \exp(-kt)\sqrt{\frac{Sct}{\pi}}.$$

...(18)

The utilized constant terminologies are given in the appendix section.

6. Numerical Results and Discussion

Figs. 2 – 21 are portrayed to explore the unsteady natural convection Casson fluid moving through an

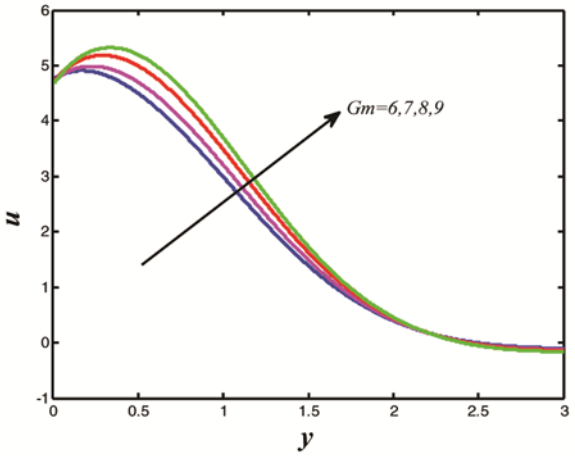

Fig. 2 — Velocity profiles for various values Gm with $M=0.6$, $Gr=0.1$, $\Omega=0.35$, $R=4, k=0.5$ $Du=0.3$, $\mathrm{Pr}=0.5$, $Sc=2.01, \alpha=30^0, \omega=\pi/4$ $Q_0=0.5, k_1=0.4$ and $t=0.5$.

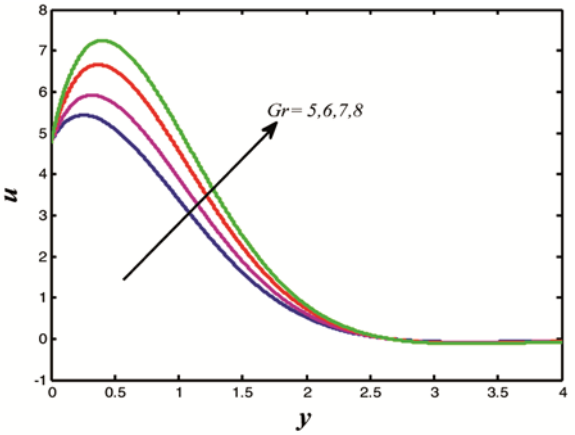

Fig. 3 — Velocity profiles for various values Gr with $M=0.6$, $Gm=5$, $\Omega=0.35$, $R=4$, $Du=0.3$ $\mathrm{Pr}=0.5$, $k=0.5$, $Sc=2.01, \alpha=30^0, \omega=\pi/4$ $Q_0=0.5, k_1=0.4$ and $t=0.5$.

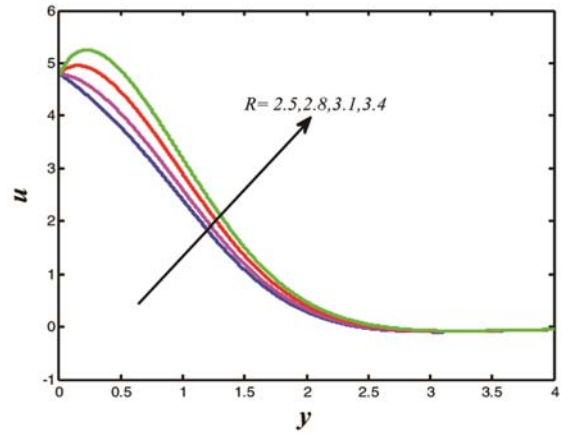

Fig. 4 — Velocity profiles for various values R with $M=0.6$, $Gm=5$, $Gr=0.1$, $Q_0=0.5$, $Du=0.3$ $k=0.5$, $k_1=0.4$, $Sc=2.01, \alpha=30^0, \omega=\pi/4$ $\mathrm{Pr}=0.5$, $\Omega=0.35$ and $t=0.5$.

inclined plate. The graphical results for velocity, fluid temperature, concentration, Sherwood number and Nusselt number are shown for various control parameters of mass Grashof number, magnetic parameter, Casson fluid parameter, thermal Grashof number, Prandtl number, radiation parameter and Dufour effect in the boundary layer region.

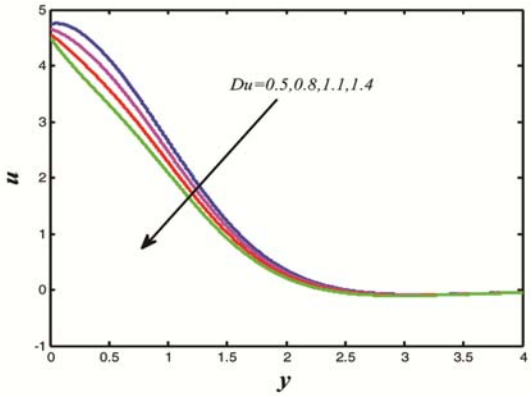

Fig. 5 — Velocity profiles for various values Du with $M=0.6$, $Gm=5$, $\Omega=0.35$, $Gr=0.1$, $R=4$ $\Pr=0.5$, $k=0.5$, $\alpha=30^0$, $\omega=\pi/4$ $Sc=2.01$, $Q_0=0.5, k_1=0.4$, and $t=0.5$.

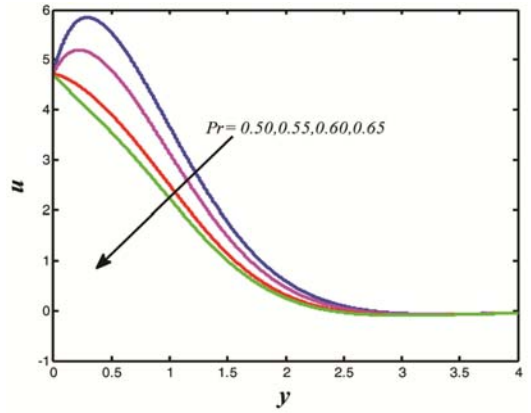

Fig. 6 — Velocity profiles for various values $\Pr$ with $M=0.6$, $Gm=5$, $\Omega=0.35$, $Gr=0.1$, $R=4$, $k=0.5$, $Sc=2.01, \alpha=30^0, \omega=\pi/4$, $Du=0.3$ $Q_0=0.5, k_1=0.4$, and $t=0.5$.

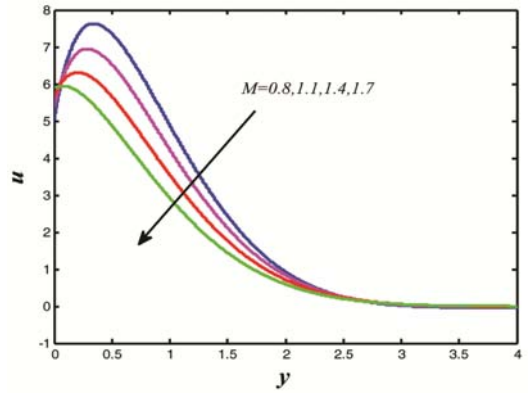

Fig. 7 — Velocity profiles for various values M with $Gm=5$, $\Omega=0.35$, $Gr=0.1$, $R=4$, $\Pr=0.5$, $k=0.5$, $Sc=2.01, \alpha=30^0$ $Du=0.3$, $\omega=\pi/4$ $Q_0=0.5, k_1=0.4$, and $t=0.5$.

6.1 Velocity profiles

Figs.2-10 demonstrates the influence of different important parameters on axial velocity. The variations in axial velocity with various values of mass Grashof number (Gm), thermal Grashof number (Gr), radiation parameter (R), Dufour effects (Du), Prandtl number (Pr), magnetic parameter (M), heat source/sink parameter (Q_0) and Casson fluid parameter (Ω). It is indicated that the velocity profiles signifying the asymptotic existence that is the

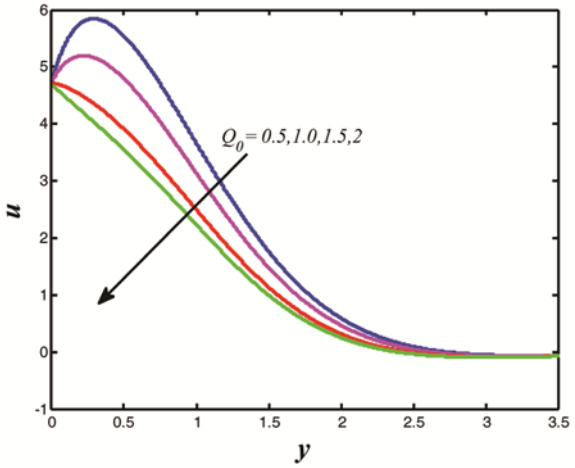

Fig. 8 — Velocity profiles for various values Q_0 with $M=0.6$, $Gm=5$, $\Omega=0.35$, $Gr=0.1$ $k_1=0.4$, $R=4$, $\Pr=0.5$, $k=0.5$, $\omega=\pi/4$ $Sc=2.01, \alpha=30^0$, $t=0.5$. and $Du=0.3$

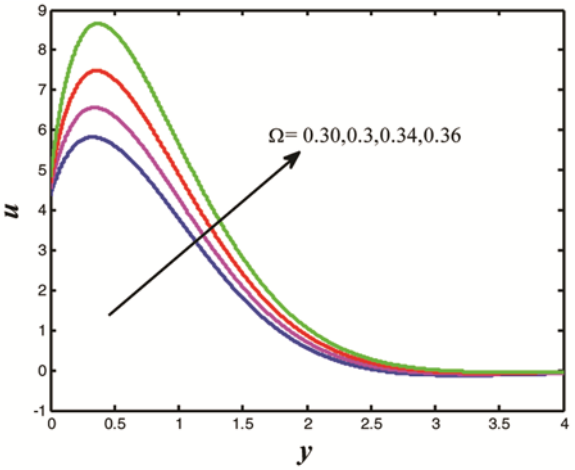

Fig. 9 — Velocity profiles for various values Ω with M = 0.6, Gm = 5 Gr = 0.1, R = 4, Pr = 0.5 Du=0.3, k=0.5, $Sc=2.01, \alpha=30^0, \omega=\pi/4$ $Q_0=0.5, k_1=0.4$ and $t=0.5$.

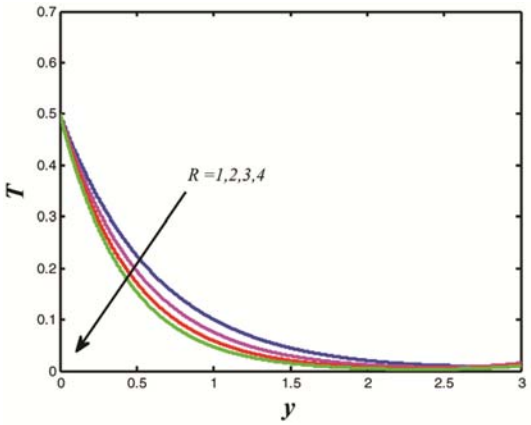

Fig. 10 — Temperature profiles for various values R with $Du = 0.3, Sc = 2.01, t = 0.5, Pr = 0.2$ and $k = 0.5$

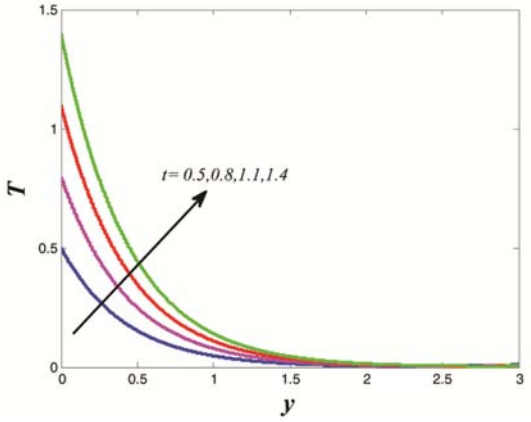

Fig. 11 — Temperature profiles for various values t with $Q_0 = 0.5 Du = 0.3, Sc = 2.01, R = 5, Pr = 0.2$ and $k = 0.5$

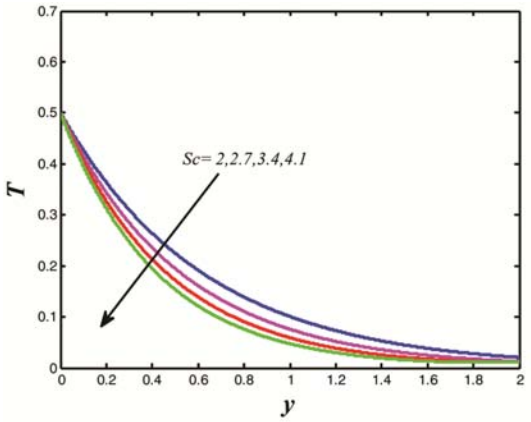

Fig. 12 — Temperature profiles for various values Sc with $Q_0 = 0.5, Du = 0.3, r = 2, R = 0.5, Pr = 0.2$ and $k = 0.5$

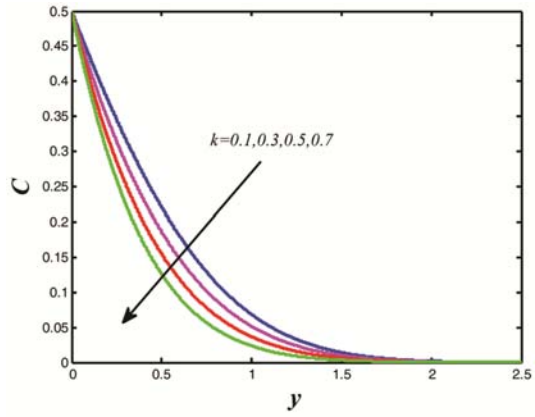

Fig. 13 — Concentration profiles for various values k with, $Sc = 2.01, t = 0.5$

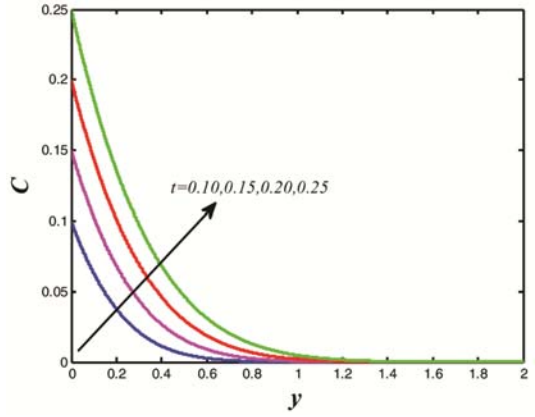

Fig. 14 — Concentration profiles for various values t with $Sc = 2.01, k = 0.5$

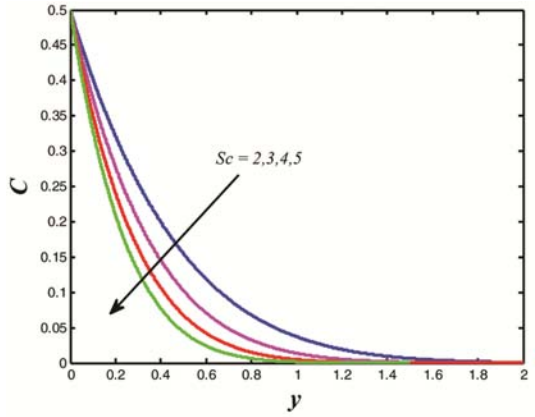

Fig. 15 — Concentration profiles for various values Sc with $k = 0.5, t = 0.5$

normal outcome on the plates with no slip flow. It's used to explore the free flow of convection in reactor cooling or to research star and planetary systems. Figure 2 and Figure 3 are found that velocity increases with raise in Gr or Gm .It indicates that the absence of the buoyance force creates the lowest fluid particle displacement, which is of great importance for water cleaning in the nuclear reactor area. Figure 4 shows that velocity increase with increasing values of R. This physically indicates that the thickening of the

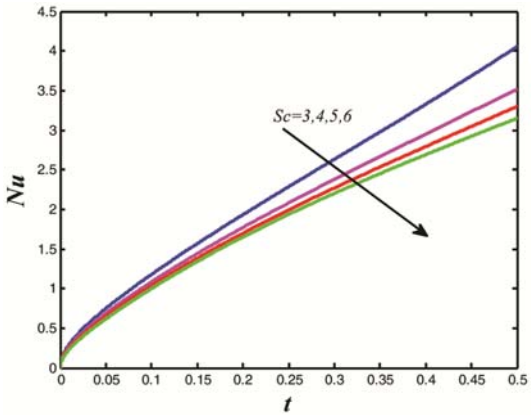

Fig. 16 — Nusselt numbers of different values *Sc* with *R* = 4, *Du* = 0.3 and Pr = 0.5

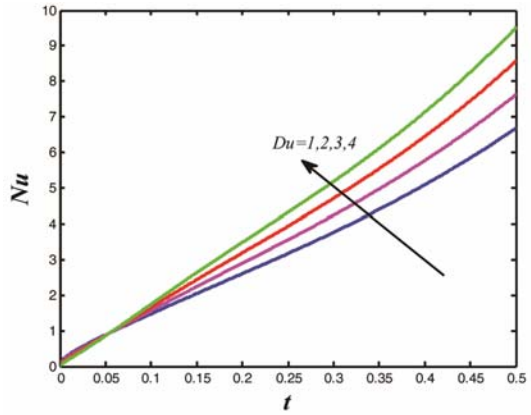

Fig. 17 — Nusselt numbers of various values *Du* with *R* = 4, *Sc* = 2.01 and Pr = 0.5

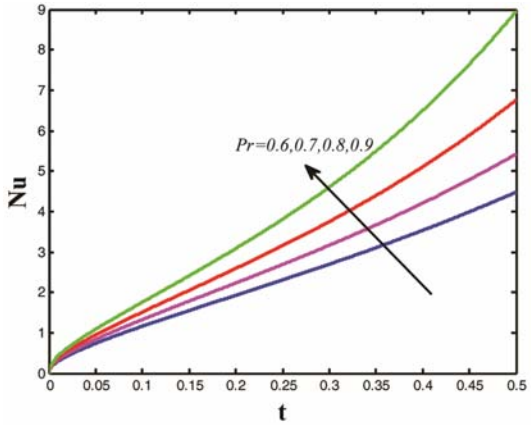

Fig. 18 — Nusselt number of various values Pr with *R* = 4, *Du* = 0.3 and *Sc* = 2.01

impulse limit layer was observed in line with the observation when radiation is involved. Figure 5 shows the Dufour effect on fluid velocity. It is mentioned that the velocities of fluid decreasing with increasing values of Dufour effect. Figure 6 shows the velocity profile for different values of Prandtl number

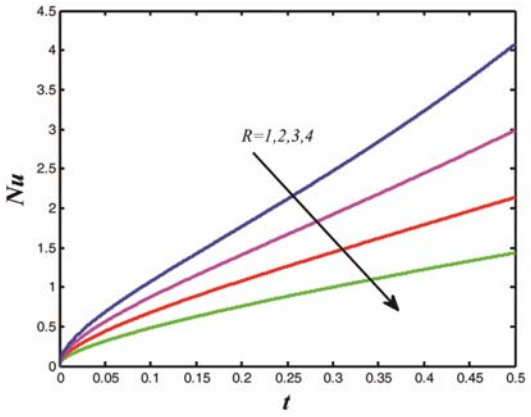

Fig. 19 — Nusselt numbers of various values *R* with Pr = 0.5, *Du* = 0.3 and *Sc* = 2.01

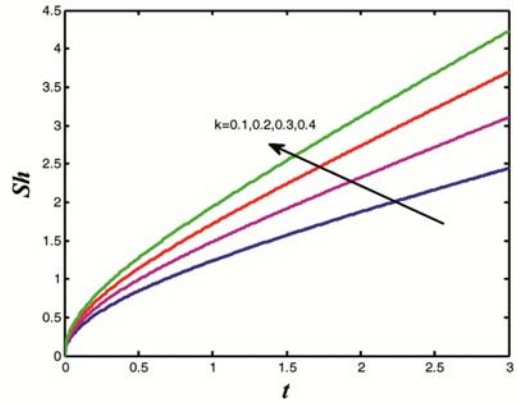

Fig. 20 — Sherwood numbers of different values *k* with *Sc* = 2.01

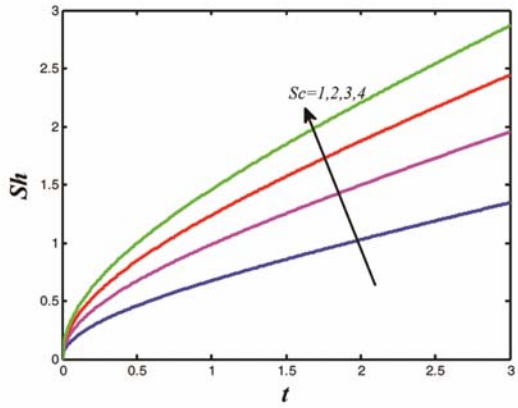

Fig. 21 — Sherwood numbers of different values *Sc* with *k* = 0.5

Pr. We found that motion of the fluid velocity decreases with increasing Prandtl number. Figure 7 represents the effect of magnetic parameter M on the velocity profile. It is observed that the fluid velocity as well as the boundary layer thickness decreases when M is increased. The magnetic field provides the Lorentz force with a resistance that induces velocity and shear stress decreases. The influence of Q_0 on the

velocity profile is shown in Figure 8. Physically, the heat supply requires heat generation from the region's surface that increases the flow field temperatures. Thus, the parameter of heat generation appears to be accelerated velocity profile. Figure 9 represents Casson fluid parameter Ω. It is found that velocity increases with increased values of Casson fluid parameter. In addition, it is noted that the fluid parameter of Casson has little effect when the fluid travels forward.

6.2 Temperature profiles

The influence of radiation parameter, time and Schmidt number on the velocity profile is illustrated in Figures 10-12. The temperature profile for different value of R is presented in Figure 10. It is investigational that increasing value of radiation parameter R with fluid temperature decreases. As radiation is accessible, the thermal boundary layer is often thickened, and the energy is diffused by radiation. Figure 11 is plotted to reveal the effects of the dimensionless time t on the temperature profile. Obviously the increasing time t the temperature also gets increases. Figure12 shows that the temperature decreases on increasing value of Sc. It is noted that the temperatures of fluid decreases with increasing values of Sc.

6.3 Concentration profile

Figure 13 indicates the concentration profiles for various parameter values for chemical reaction. The chemical reaction is then observed to decrease the concentration distribution. Figure 14 indicates that the increasing values of t the concentration increases. Figure 15 shows that the concentration profiles for different values of Sc .We have to found that concentration decreases with increasing values of Sc.

6.4 Nusselt number and Sherwood number profiles

The Nusselt and Sherwood numbers tend to find the rate of the heat transmission and the rate of mass transmission on the accelerating plate. It can be used for the investigation of the free convection flow in nuclear reactor cooling or for the study of star and planetary systems. Figure 16 exhibits the Nusselt number for different values of Sc. It is observed that Nusselt number decreases with increment in Sc. Figure 17 shows the effect of Du on Nusselt number. It is observed that Nusselt number increases with increasing Du. Figure 18 shows the effect of $\Pr$ on Nusselt number. It is seen that Nusselt number increases propensity with $\Pr$. Figure 19 shows the effect of Radiation effect R on Nusselt number. It is seen that Nusselt number increases with increasing values of radiation effect. Figure 20 shows the effect of Sc on Sherwood number. It is observed that Sherwood number increases with increased values of Sc.

7. Conclusion

In this analysis, the exact solutions and numerical results for the unsteady natural Casson convective fluid moving through an inclined plate were considered. The fluid temperature, and concentration closed by the Laplace transform technique was used to find the numerical solution. The results on, temperature, velocity, concentration, Nusselt number and Sherwood number of the related parameters can be obtained graphically. The following are the most critical concluding observations:

- With improved values of thermal Grashof number and Mass Grashof number, the fluid velocity increases.
- If the different values of the Dufour effect increases, the fluid velocity gets decreases.
- For large values of parameter k, velocity and boundary layer thickness also increased.
- Velocity increasing with Various increasing values of the of Casson fluid parameter Ω
- Temperature decreases while the Schmidt number Sc got increasing values.
- Concentration decreases with increase in Schmidt number Sc .
- Nusselt number is increases with increasing values of $\Pr$, Du and R .
- Sherwood number is increases with increasing value in Schmidt number Sc and *K*.

Nomenclature

B_0 -Uniform magnetic field

k_1 - Permeability parameter

$\bar{k}_1$ -Permeability of porous medium

$\bar{C}$ - Species concentration

C_w -Concentration of the plate

$\bar{C}_\infty$ -Concentration of the fluid far away from the plate

C -Dimensionless concentration

C_p -Specific heat at constant pressure

Du - Dufour effect

D_m -Coefficient of mass diffusivity

g -Acceleration due to gravity

Gr -Thermal Grash of number

Gm - Mass Grash of number

M -Magnetic field parameter

Nu - Nusselt number

$\Pr$ - Prandtl number

q_r - Radiative heat fluxes in the - $\overline{y}$ direction

R -Radiation parameter

Sc -Schmidt number

T -dimensionless fluid Temperature

$\overline{T}_w$-Temperature of the plate

$\overline{T}_\infty$-Temperature of the fluid far away from the plate

t -Time

$\overline{t}$ - Dimensionless time

$\overline{u}$ -Velocity of the fluid in the $\overline{y}$ direction

u_0-Velocity of the plate

u-Dimensionless velocity

$\overline{y}$ -Coordinate axis normal to the plate

y -Dimensionless Coordinate axis normal to the plate

k -Thermal conductivity of the fluid

α -Thermal diffusivity

β_T - Thermal expansion volumetric coefficient

β_C-Concentration expansion of volumetric coefficient

μ - Viscosity coefficient

v - Kinematic viscosity

ρ -Density of the fluid

σ - Electric conductivity

Q_0 - Dimensionless heat source

θ - Inclination angle from the vertical direction

Ω -Casson fluid parameter

Appendix

$$a=\frac{\left(M^2k_1+1\right)}{k_1}\quad,\ b=\left(\frac{1}{1+\Omega}\right),$$

$$a_1=\frac{Du\,\Pr k}{\Pr-Sc},a_2=\frac{Sc\,k-R-Q_0\,\Pr}{Sc-\Pr},$$

$$a_3=\frac{Du\,Sc\,\Pr}{\Pr-Sc},a_4=\frac{a_1}{a_2^2},a_5=\frac{a_1}{a_2},a_6=\frac{a_3}{a_2},$$

$$a_7=\frac{Gr\cos\alpha}{1-b\,\Pr},a_8=\frac{bR-a+bQ_0\,\Pr}{b\,\Pr-1},$$

$$a_9=\frac{a_7}{a_8^2},a_{10}=\frac{a_7}{a_8},a_{11}=\frac{a_7a_5}{a_8^2},a_{12}=\frac{a_7a_5}{a_8},$$

$$a_{13}=\frac{-a_7a_4(a_2+a_8)}{a_2a_8^2},a_{14}=\frac{a_7a_4}{a_8},$$

$$a_{15}=\frac{a_7a_4}{a_2(a_8-a_2)},a_{16}=\frac{a_7a_4a_2}{a_8^2(a_2-a_8)},a_{17}=\frac{a_7a_3}{a_2a_8},$$

$$a_{18}=\frac{a_7a_3}{a_2(a_2-a_8)},a_{19}=\frac{a_7a_3}{a_8(a_8-a_2)},$$

$$a_{20}=\frac{Gr\cos\alpha}{1-bSc},a_{21}=\frac{bSc\,k-a}{bSc-1},a_{22}=\frac{a_{20}\,a_4}{a_{21}},$$

$$a_{23}=\frac{a_{20}\,a_5}{a_{21}^2},a_{24}=\frac{a_{20}\,a_5}{a_{21}},a_{25}=\frac{a_{20}\,a_4}{a_2-a_{21}},$$

$$a_{26}=\frac{a_{20}\,a_6}{a_{21}},a_{27}=\frac{a_{20}\,a_6}{a_{21}-a_2},a_{28}=\frac{Gm\cos\alpha}{1-bSc},$$

$$a_{29}=\frac{a_{28}}{a_{21}^2}a_{30}=\frac{a_{28}}{a_{21}},$$

$$A_1=(a_9-a_{11}-a_{13}+a_{17}+a_{22}+a_{23}-a_{26}+a_{29}),$$

$$A_2=(-a_{10}+a_{12}-a_{14}-a_{24}-a_{30}),$$

$$A_3=(-a_{15}+a_{18}+a_{25}+a_{27}),A_4=(-a_9+a_{11}-a_{16}+a_{19}),$$

$$A_5=(-a_{22}-a_{23}-a_{25}+a_{26}-a_{27}-a_{29}),$$

$$A_6=(-a_9+a_{11}+a_{13}-a_{17}),A_7=(a_{10}-a_{12}+a_{14}),$$

$$A_8=(a_{15}-a_{18}),A_9=(a_9-a_{11}+a_{16}-a_{19}),$$

$$A_{10}=(-a_{22}-a_{23}+a_{26}-a_{29}),A_{11}=(a_{24}+a_{30}),$$

$$A_{12}=(-a_{25}-a_{27}),A_{13}=(a_{22}+a_{23}+a_{25}-a_{26}+a_{27}+a_{29})$$

References

1 Steffe J F, *Rheological methods in food process eng*, *Freeman press*, 1996.

2 Ferry J D, *Viscoelastic Properties of Polymers*, *Wiley NewYork*, (1980).

3 Ramesh K, Tripathi D, Anwar Beg O & Kadir A, *Iran J Sci Technol Trans Mech Eng*, 43 (2019) 675.

4 Prakash J, Ramesh K, Tripathi D & Kumar R, *Microvas Res*, 118 (2018) 162.

5 Tripathi D, Yadav A, Anwar Beg O & Kumar R, *Microvas Res*, 117 (2018) 28.

6 Prakash J, Reddy M G, Tripathi D & Tiwari, *Nanotechnol Energy Environ Eng*, (2020) 185.

7 Casson N, A *flow equation for the pigment oil suspensions of the printing ink type*, in: Mills C C (Ed), Rheology of Disperse Systems, Pergamon, New York Oxford, (1959) 84.

8 Alfven H, *Nature*, 150 (1942) 405.

9 Hartmann J, Hg-dynamics I theory of the laminar flow of an electrically conductive liquid in a homogenous magnetic field, Det Kal Danske Videnskabernes Selskab (Mathematisk - Fysiske Meddeleser) 15 (1937) 1.

10 Su X & Yin Y, *J Magn Magn Mater*, 484 (2019) 266.

11 Okuyade W I A, Abbey T M & Gima-Laabel A T, *Alexandria Eng J*, 57 (2018) 3863.

12 Tassaddiq A, *Chaos Solutions Fractals*, 123 (2019) 341.

13 Venkata Ramudu A C, Anantha Kumar K, Sugunamma V & Sandeep N, *J Thermal Analys Calorimetry* (2019), https://doi.org/10.1007/s10973-019-08776-7.
14 Kothandapani M & Prakash J, *J Nanofluids*, 5 (2016) 363.
15 Bharathi V, Vijayaragavan R & Prakash, *Heat Transfer*, (2020) https://doi.org/10.1002/htj.21860.
16 Narla V K & Tripathi D, *Microvas Res*, 123 (2019) 25.
17 Ranjit N K, Shit G C & Tripathi D, Microvas Res, 117 (2018) 74.
18 Ravikumar R, Arul Freeda Vinodhini G & Prakash J, *Int J Eng Adv Technol*, 9 (2019) 5384.
19 Pramanik, *Ain Shams Eng J*, 5 (2014) 205.
20 Prasad D V K, Chaitanya G S K & Raju R S, *Res Eng*, 3 (2019) 100019.
21 Arthur E M, Seini I & Bortey B Y, *J Appl Math Phys*, 3 (2015) 713.
22 Vijayaragavan R & Bharathi V, *Int J Res Adv Tech*, 6 (2018) 2617.
23 Kataria R & Patel H R, *Alexandria Eng J*, 55 (2016) 2125.
24 Raza J, *Propul Power Res*, 8 (2019) 138.
25 Palaniammal S & Saritha K, *Front Heat Mass Trans*, 10 (2018).
26 Vijayaragavan R & Bharathi V, *J Emerg Technol Innov Res*, 5 (2018) 554.
27 Vijayalakshmi P, Rao G S, Animasaun I L & Sivaraj R**,** *Appl Math Sci Comput Trends Math*, (2019) 117.
28 Ajayi T M, Omowaye A J & Animasaun I L, *Hind J Appl Math*, 13 (2017).
29 Hamida M, Usman M, Khan Z H, Haq R U & Wang W, *Int Commun Heat Mass Trans*, 108 (2019) 104284.
30 Shateyi S, Mabood F & Lorenzini G, *Heat Mass Trans J Eng Thermo Phys*, 26 (2017) 39.
31 Mackolil J & Mahanthesh B, *J Comput Design Eng*, 6 (2016) 593.
32 Rehman K U, Malik A A, Malik M Y, Sandeep N & Saba N U, *Res Phys*, 7 (2017) 2997.
33 Neeraja A, Renuka D R L V, Devika B, Naga R V & Krishna M M, *Res Eng*, 4 (2019) 100040.
34 Renuka P, Ganga B, Kalaivanan R & Abdul H A K, *Appl Comput Mech*, 6 (2020) 296.
35 Vijayaragavan R & Bharathi V, *Int J Res Eng Appl Manage*, 05 (2019) 2454.
36 Das M, Mahanta G, Shaw S & Parida S B, *Heat Trans Asian Res*, 48 (2019) 1761.